Interfacial/foaming properties and antioxidant activity of a silkworm (*Bombyx mori*) pupae protein concentrate

Manuel Felix[a,*], Carmen Bascon[a,b], Maria Cermeño[b], Richard J. FitzGerald[b], Julia de la Fuente[a] and Cecilio Carrera-Sánchez[c]

[a] *Departamento de Ingeniería Química, Escuela Politécnica Superior, Universidad de Sevilla, 41011 Sevilla, Spain*

[b] *Department of Biological Sciences, School of Natural Sciences, University of Limerick, Ireland*

[c] *Departamento de Ingeniería Química, Facultad de Química, Universidad de Sevilla, 41012 Sevilla, Spain.*

---

*__Manuel FELIX__

Departamento de Ingeniería Química, Escuela Politécnica Superior, Universidad de Sevilla, 41011 Sevilla, Spain.

E-mail: mfelix@us.es

Phone: +34 954557179; fax: +34 954556447.

Abstract

The current consumer demand for healthier diets, the growing interest in the search for new sources of protein, and the desire to reduce the negative effects on the environment have increased interest in the study of insect proteins. The present study focused on the technofunctional characteristics (interfacial and foaming properties) and the *in-vitro* antioxidant activity of a protein concentrate obtained from silkworm (*Bombyx mori*) pupae (SPC). The isoelectric point of the SPC was close to pH 4.0-5.0 as determined by protein solubility and z potential analysis. Given that the SPC had solubilities of ~50 % and z potentials of ~20 mV at pH 2.0 and 8.0, it was decided to further study SPC properties at these pH values.

The supernatant obtained after adjustment of SPC to pH 8.0 showed higher ($p < 0.05$) antioxidant activity than those at pH 2.0 when analysed by the ferric reducing antioxidant power (FRAP) assay (168.0 ± 3.0 Vs. 43.5 ± 8.1 μmol Trolox Eq. $\cdot g^{-1}$ protein). However, no significant differences in antioxidant activity were found between pH 2.0 and 8.0 when using the oxygen radical absorbance capacity (ORAC) assay (1826.0 ± 131.9 vs. 1659.2 ± 46.8 μmol Trolox Eq. g^{-1} protein). The interfacial properties of SPC were determined at pH 2.0 and 8.0 during protein adsorption and after reaching the pseudo equilibrium state by means of dilatational and interfacial shear rheology following by foaming capacity and stability analyses. Faster adsorption kinetic values were obtained at pH 8 ($k_D^* = 69.2 \pm 0.4$ Vs. $29.5 \pm 0.9\, mN/m \cdot s^{-1/2}$ at pH 2.0). However, lower kinetic values at pH 2.0 increased the elastic behaviour of the viscoelastic interfacial film formed ($E'_s \sim 30$ mN/m at pH 2.0 Vs. $E'_s \sim 20$ mN/m at pH 8.0), which can be related with the higher protein sizes found at pH 2.0. These rearrangements of the SPC components appeared to increase its foaming capacity, whereas the foaming capacity of SPC adjusted to pH 8.0 was minimal.

Keywords: *Bioactivity; Interfacial Shear Rheology; Dilatational measurements; Protein adsorption*

1. Introduction

An increased consumer demand for healthy food products has been well documented. A healthy diet must provide all necessary nutrients, e.g., protein, lipid, carbohydrate, vitamins and minerals in adequate quantities according to individual needs (Boland et al., 2013). Meat, fish, seafood, dairy, eggs and legumes are considered as conventional sources of dietary protein. However, due to increases in worldwide population, novel and sustainable protein sources are required in order to meet the upcoming demand. In particular, the food industry is focused on using protein surpluses and by-products for the development of protein rich ingredients (Bruinsma et al., 2009).

Edible insects have therefore received much interest in recent years. Insect farming is environmentally sustainable due to its low extent of consumption of natural resources and its low impact on carbon footprint (Oonincx et al., 2011). Moreover, insects possess an adequate amino acid composition as well as a suitable lipid profile for human nutrition (Kim, Setyabrata, Lee, Jones, & Kim, 2016). In addition, European Regulation 2015/2283 authorises the use of specific novel ingredients such as insects for human consumption (Sjödin, 2018).

Silkworms are highly efficient silk producers. Among the different species, *Bombyx mori*, *Antheraea pernyi* and *Bombyx eri* are widely used in sericulture (Mahendran, Ghosh, & Kundu, 2006; Prasad et al., 2005; Reddy, Abraham, & Nagaraju, 1999). China and India are the world's largest silk producers with around 60 % of total world silk, corresponding to 16,380 metric tons (Koeppel & Holland, 2017). After the collection of silk from the cocoon, silkworm pupae (rich in protein, lipid and minerals) are discarded and are considered as waste products. However, silkworm pupae is composed of ~55 % protein and ~32% lipid (Tomotake, Katagiri, & Yamato, 2010). Silkworm proteins are rich in essential amino acids such as valine, methionine and phenylalanine which could help meet human dietary requirements (Tomotake et al., 2010).

The antioxidant activity of silkworm proteins has been previously reported. A protein rich fraction extracted from the larvae of *Bombyx mori L*. by ammonium acetate precipitation showed antioxidant 2,2-Diphenyl-1-picrylhydrazyl ($DPPH^{\bullet}$), 2,2'-azino-bis(3-ethylbenzothiazoline-6-sulphonic acid) ($ABTS^{+\bullet}$) and superoxide anion radical scavenging activity (Takechi, Wada, Fukuda, Harada, & Takamura, 2014). High antioxidant activity was also observed in an aqueous protein extract from *B. mori* pupae (Chatsuwan, Puechkamut, & Pinsirodom, 2018). Furthermore, simulated gastrointestinal digestion of *B. mori* protein released hydrolysates which had significantly higher antioxidant activity than the parent protein due to the generation of bioactive peptides (Wu, Zhao, & Yang, 2011). Insect-derived peptides have also shown other bioactive properties related to key physiological markers associated with antihypertensive, antimicrobial and hepatoprotective activities (Jena, Kar, Kausar, & Babu, 2013; Kumar, Dev, & Kumar, 2015; Lieselot Vercruysse, Guy Smagghe, Herregods, & Van, 2005; Xia, Ng, Fang, & Wong, 2013). Therefore, the use of silkworm protein as food ingredients could have a beneficial effect in human health.

Proteins are surface active agents which are able to adsorb at oil/water (O/W) and air/water (A/W) interfaces, forming interfacial layers (Caro et al., 2005; Rodríguez Patino, Carrera Sánchez, Molina Ortiz, Rodríguez Niño, & Añón, 2004). Dispersed food systems such as emulsions or foams can be stabilized by proteins. Many food products exists as foams, e.g., mousses, creams, cakes, muffins, among others (Martinez, Carrera Sánchez, Rodríguez Patino, & Pilosof, 2012), where foam formation and stability are controlled by the dynamics of the adsorbed protein layer at the interface (Ruiz-Henestrosa, Carrera-Sanchez, & Rodriguez-Patino, 2008a).

The aim this work was to assess the techno-functional and *in vitro* antioxidant properties of a protein concentrate obtained from silkworm (*B. mori*) pupae at two different pH values (2.0 and 8.0). The behaviour of the SPC at the A/W interface was characterised by dilatational and

interfacial shear measurements (during protein adsorption and after reaching the quasi-equilibrium state). Furthermore, foams were formed at pH 2.0 and 8.0 and were then characterised. The interfacial properties were correlated with the results obtained for the foaming properties (foaming capacity and foam stability). The antioxidant capacity of the protein isolate was assessed using the oxygen radical absorbance capacity (ORAC) and ferric reducing antioxidant power (FRAP) assays

2. Material and methods

2.1. Materials

The silkworm protein concentrate (SPC) used in this study was supplied by FeedStimulants (Amsterdam, the Netherlands). Chemical reagents (i.e., HCl, NaOH, NaH_2PO_4) were purchased from Sigma–Aldrich Company (St. Louis, USA). The solutions were prepared using Milli-Q grade water.

2.2.Sample preparation

SPC was defatted using n-hexane (to avoid the influence of lipid on the results obtained). SPC protein solutions (2 wt.%) were prepared at pH 2.0 and 8.0 using 50 mM of phosphate and Trizma-base buffer solutions, respectively. Following 30 min stirring the samples were centrifuged for 15 min at 15,000×g using the BL-S centrifuge (Selecta, Barcelona, Spain). The pH 2.0 and 8.0 supernatants were then collected and store at 4 ºC for further analysis.

2.3. Proximate analysis of SPC

The Dumas method was used for determination of the protein content (% N x 6.25) using a LECO CHNS-932 nitrogen micro analyser (Leco Corporation, St. Joseph, MI, USA). The lipid, moisture and ash contents of the SPC protein system was determined according to A.O.A.C. approved methods (2000).

2.4.Sample characterisation

2.4.1. Measurement of protein solubility

The solubility of the SPC protein system was determined using the Lowry et al. method (1951) for protein determination, with some modifications (Markwell, Haas, Bieber, & Tolbert, 1978). Protein dispersions (1 mg/mL) were prepared as a function of pH (between 2.0 and 10.0) using buffers at pH 2, 3, 4, 5, 6, 7, 8, 9 and 10 (phosphate, chloroacetate, acetate, pyridine, phosphate, TRIS, tricine and ethanolamine buffers). Following 30 min stirring the pH was re adjusted if necessary and samples were centrifuged for 15 min at 15,000×g using a BL-S centrifuge (Selecta, Barcelona, Spain). Supernatants were collected and an aliquot was taken for z-potential experiments (see section 2.2.3). The remaining supernatant was subjected to protein solubility determination by Lowry et al. with some minor modifications (Markwell et al., 1978) method. Briefly, supernatants (0.1 mL) at 1mg/mL of SPC protein were mixed with 3 mL of a solution containing sodium carbonate (2%), sodium dodecyl sulphate (1%), potassium sodium tartrate (1.6%) and Copper(II) sulphate (0.04 %). Subsequently, Folin-ciocalteu reagent (1N) was added and samples were incubated for 40 min. Absorbance was measured at 660 nm, bovine serum albumin (BSA) protein was used as standard. Protein solubility was determined in triplicate.

2.4.2. Z-potential

Z-potential measurements of aqueous protein dispersions were determined using a Zetasizer Nano Z from Malvern Instruments (Malvern, UK). Protein dispersions prepared at different pH values (from 2 to 10) at 0.1 wt.% using the same buffers as in 2.3.1 section. The Zetasizer device allows measurement of the global charge state of a protein, the Smoluchowski equation (1.5 for F_{ka} value) was used for these measurements. Z-potential was determined in triplicate.

2.4.3. SDS-PAGE

The molecular masses of the proteins within the SPC soluble fractions at pH 2.0 and 8.0 were determined using SDS-PAGE. A continuous 4-20 % acrylamide gradient gel (Bio-Rad, Hemel Hempstead, UK) was used. A total of 15 mg of soluble SPC protein was loaded into each lane. A wide-range molecular weight marker from 6 to 200 kDa (Sigma Aldrich) was used. Electrophoresis was run at a constant voltage of 200 V. The gel was stained with Coomassie Blue for 1 h and destained with a solution containing 10 % methanol and 10% acetic acid in water.

2.4.4. Antioxidant properties

The antioxidant activity of the soluble protein fractions (supernatants) obtained at pH 2.0 and 8.0 were determined using the FRAP and ORAC assays as previously described by Cermeño et al. (2016). All measurements were carried out using a microplate reader (BioTek Synergy HT, USA). The FRAP and ORAC activities were expressed as µmol of Trolox equivalents (TE) per gram of SPC protein. All measurements were carried out at least in triplicate.

2.5.Interfacial characterization

2.5.1. Determination of interfacial tension at equilibrium

Surface-tension measurements were performed to determine the saturation concentration at the A/W interface using a Sigma D701 tensiometer (KSV, Helsinki, Finland) based on the Wilhelmy method. The measurements were carried out at different SPC concentrations (0.1, 0.25, 0.5, 0.75, 1.0, 2.0, 3.0, 4.0 and 5.0 wt.%) and at two pH values (2.0 and 8.0) which was achieved by adjusting with 50 mM of phosphate and TRIZMA-base buffer solutions, respectively. The interfacial tension was measured during 15 min on reaching a constant experimental value.

2.5.2. Pendant droplet measurements

Pendant droplet measurements were carried out in order to monitor the adsorption process of the supernatants (obtained at pH 2.0 and pH 8.0) of the SPC system at A/W interface. Transient and stationary surface tension and dilatational measurements were performed using a TRACKER pendant-droplet tensiometer (IT Concept, France). Briefly, an axisymmetric drop (8 μL) was formed at the tip of the needle of a vertically placed syringe. The droplet profile was digitized and analysed through a CCD camera coupled to a video image profile digitizer. Droplet profiles were processed according to the Laplace equation as described by Castellani et al. (2010).

In addition, the viscoelastic moduli of the protein adsorption at the A/W interface were determined at 10% strain amplitude and at 0.1 Hz. After reaching the quasi-equilibrium state (after 180 min), frequency sweep tests were performed (from 0.0075 to 0.1 Hz). All experiments were carried out, at least in triplicate at 20.0 ± 0.1 °C.

The apparent diffusion coefficient (k_D^*) and the first-order constant (k_A) associated with the kinetics of interfacial protein film formation were calculated according to Perez et al. (2009). k_D^* was calculated according with Eq. 1:

$$\Pi = k_D^* \, [t]^{1/2} \qquad (3)$$

where according to Ward and Tordai (1946) equation, $k_D^* = \frac{2}{\sqrt{\pi}} c_0 \kappa T [D]^{1/2}$.

Moreover, k_A was calculated according to the following first-order phenomenological equation:

$$\ln \frac{\Pi_f - \Pi(\mathrm{t})}{\Pi_f - \Pi_0} = -k_A \cdot t \qquad (4)$$

where Π_f, $\Pi(\mathrm{t})$ and Π_0 are the surface pressures at the final adsorption time, at any time (t), and at the initial time (0), respectively.

2.5.3. Interfacial shear rheological properties

Surface shear measurements were carried out during the process of protein adsorption and after reaching the quasi-equilibrium state (i.e., after 180 min) using a double-wall-ring geometry

(DWR) connected to a highly sensitive magnetic air bearing stress-controlled rheometer (DHR-3, TA Instruments, USA) (Vandebril, Franck, Fuller, Moldenaers, & Vermant, 2010). Stress swept tests were performed prior to all measurements to determinate the linear viscoelastic region (LVR). Time sweep tests were carried out during protein adsorption at 0.1 Hz, whereas the mechanical spectra were obtained by means of frequency sweep tests (from 0.1 to 1 Hz). All experiments were carried out at 20.0 ± 0.1 °C. Moreover, the Boussinesq number (Bo) was calculated for all systems studied to evaluate the contribution of the bulk to the interfacial small amplitude oscillatory shear measurements (i-SAOS) (Eq. 1):

$$Bo = \frac{\eta_s}{a \cdot \eta_b} \qquad \text{(Eq. 1)}$$

where a is a characteristic length (0.07 mm for DWR geometry), η_s the interfacial shear viscosity and η_b the bulk viscosity.

Bo was greater than 100 in all cases (Bo > 100). This indicates that the responses obtained can be attributed to the contribution of the interfacial layer (Vandebril et al., 2010).

2.6. Foam formation and foam stability

Determination of the foaming properties (foam formation and foam stability) was performed using a Foamscan instrument (Teclis-It Concept, Longessaigne, France). The foam was generated by blowing nitrogen gas at a flow of 45 mL/min through a porous glass filter (0.2 μm) at the bottom of a glass tube where 20 mL of the aqueous foaming solution (25.0 ± 0.5ºC) was placed in the experimental set-up. In all experiments, the foam was allowed to reach a volume of 120 mL. Once the foam volume reaches 120 mL and the device stop bubbling, the device measures the foam decay (foam stability). The evolution of the foam was analysed by means of conductivity and optical images taken with a CCD CAM, 2X zoom, every 100 s at 10 cm foam height. Several parameters were calculated in order to evaluate the foaming capacity and stability. For the former, the overall foaming capacity (OFC) was determined as the slope

of the foam volume curve until the end of the bubbling process. The foaming capacity (FC), a measure of gas retention in the foam, was calculated as follows:

$$FC = \frac{V_{foam(f)}}{V_{gas\,(f)}} x100 \qquad \text{(Eq. 2)}$$

where $V_{foam(f)}$ and $V_{gas(f)}$ were the final foam volume and the final gas volume injected, respectively

The relative foam conductivity ($CF, \%$), is a measure of the foam intensity and was calculated by Eq. (3):

$$CF = \frac{C_{foam}}{C_{liq}} x100 \qquad \text{(Eq. 3)}$$

where C_{foam} and C_{liq} were the final foam and liquid conductivity, respectively.

The foam maximum density (MD), a measure of liquid retention in the foam, was also determined (Eq. 4):

$$MD = \frac{V_{liq\,(i)} - V_{liq\,(f)}}{V_{foam\,(f)}} x100 \qquad \text{(Eq. 4)}$$

Where $V_{liq\,(i)}$ corresponds to the initial liquid volume, $V_{liq\,(f)}$ corresponds to the final liquid volume and $V_{foam\,(f)}$ corresponds to the final volume of the foam.

The static foam stability was determined from the volume of liquid drained from the foam over time. The foam half-life ($t_{1/2}$) refers to the time needed to drain half of the volume of liquid from the foam (Rodríguez-Patino, Niño, & Gómez, 1997).

Additionally, the evolution of the bubble size change in the foam was also determined by a second CCD camera set which allowed capture of air bubble size variation every 5 s.

2.7. Statistical analysis

234 At least three replicates of each measurement were carried out. Measurement variation was
235 determined by means of standard deviation. Significant differences ($p < 0.05$) were analysed
236 by means of ANOVA tests (Excel statistical package).

237 ## 3. Results and discussion

238 ### *3.1 Protein system characterisation*

239 #### *3.1.1 Protein composition*

240 The proximate composition of the SPC before and after defatting is shown in Table 1. Before
241 defatting, contained 50.5 wt.% protein, 28.9 ± 0.2 wt.% lipid, 6.6 ± 0.8 wt% ash and 8.9 ± 0.1
242 wt % moisture and, whereas after defatting, contained 71.0 wt.% protein, 28.9 ± 0.2 wt.% lipid,
243 12.5 ± 1.4 wt% ash and 9.3 ± 1.1 wt % moisture. The protein content of SPC was higher than
244 that reported for legumes (Boye, Zare, & Pletch, 2010), meat (Multari, Stewart, & Russell,
245 2015) or cereals (Zhai, Wang, & Han, 2015). Similar results for protein content were previously
246 obtained for a silkworm pupae protein concentrate (David-Birman, Moshe, & Lesmes, 2019;
247 Tomotake et al., 2010). The lipid content was similar to that reported for *B.mori* pupae flour.
248 Due to the high lipid content, the protein system was defatted using n-hexane at room
249 temperature in order to avoid interference from the lipid on the technofunctional and bioactive
250 properties. The carbohydrate content, estimated by difference, reached 7.2 wt.%. Wimer (1969)
251 indicated that glycogen was the main carbohydrate present for energy storage in the fly
252 (*Phormia regina)* during its pupae state.

253 #### *3.1.2 Protein solubility and Z-potential*

254 The protein solubility and Z-potential of SPC as a function of pH (from pH 2.0 to 10.0) are
255 shown in Figure 1. The results indicate a moderate protein solubility which ranged from 31.6 ±
256 1.2 % at pH 5.0, to 60.1 ± 2.5 % at pH 10.0. Z-potential analysis indicated that the isoelectric

point (IEP) of the SPC protein system was c.a. pH 4.0. This indicate that the net surface charge of the SPC sample was zero at pH 4.0 and that this pH value should ideally be avoided when using this protein system for the stabilization of interfaces (Schwenzfeier, Lech, Wierenga, Eppink, & Gruppen, 2013). The IEP (c.a. pH 5.5) obtained using the Lowry protein quantification approach (which corresponds to the minimum of solubility) differs from the value obtained by Z-potential (which corresponds to zero surface charge). This difference may be related to the presence of carbohydrates (20.6 %), which can influence the Z-potential in a protein system (Spada, Marczak, Tessaro, & Cardozo, 2015). The solubility (c.a. 50 wt.%) and surface charge (c.a. +/- 20 mV) values of SPC system adjusted to pH 2.0 and 8.0, respectively, may be considered suitable for the development of food products such as foams or emulsions (McClements, 2015). Therefore, further characterisation of aqueous protein solutions was carried out on the SPC system adjusted to pH 2.0 and 8.0.

3.1.3 Protein profile

Fig. 2 shows the protein profiles of the SPC protein system supernatants obtained at pH 2.0 and 8.0 as obtained by SDS-PAGE. Low-intensity bands were obtained regardless of the pH value, which is in agreement with the data in Fig.1 showing similar overall protein solubility at pH 2.0 and 8.0. However, the electrophoretic profiles show that pH affects protein profile of the soluble protein present in the SPC protein concentrate. At pH 2.0, supernatants of the SPC generally had higher intensity protein bands than in the non-adjusted SPC (pH 6.3) and in the supernatant of the SPC sample adjusted to pH 8.0. At pH 2.0 the SPC supernatant had distinct protein bands around 45, 36 and 30 kDa, as well as two high intensity bands of approx. 24 and 14 kDa which were not visible when analysing the supernatant of the sample which was adjusted to pH 8. The electrophoretic profile of aqueous silkworm pupae proteins has been previously reported showing protein bands between 75 and 6.5 kDa where high molecular bands were related to albumen. Protein bands around 23 kDa were associated to glutelin, bands at 15

kDa to prolamin, and bands around 5 kDa to globulin (Chatsuwan et al., 2018). Therefore, the presence herein of bands at 24, 14 and 6 kDa were previously attributed to the presence of albumen, glutelin and globulin, respectively. These results are also in agreement with those of Wang et al. (2011) reported on silkworm pupae proteins.

3.1.4 Antioxidant properties of SPC

Table 2 shows the antioxidant properties of the SPC protein supernatants (obtained at pH 2.0 and 8.0), using the ORAC and FRAP assays. SPC at pH 2.0 had numerically lower mean ORAC values than at pH 8.0, however, these differences were not significant different ($p > 0.05$). The ORAC values obtained were 16959.2 ± 46.8 and 1826.0 ± 131.9 μmol TE g^{-1} SPC protein for pH 2.0 and 8.0, respectively. Similar results were observed in *Bombyx mori* pupae hydrolysed with Alcalase showing ORAC values of 1,950 μmol TE g^{-1} (Liu, Wan, Liu, Zou, & Liao, 2017) The antioxidant activity as measured by the FRAP assay displayed values of 43.5 ± 8.1 and 168.0 ± 3.0 μmolTE g^{-1} SPC protein for pH 2.0 and 8.0, respectively. The lower values observed at pH 2.0 may be related to differences in protein surface charge. The positive net charge of SPC at this pH (Fig. 1) may avoid interactions between the ferric ion and the protein, leading to low FRAP values (Marathe, Rajalakshmi, Jamdar, & Sharma, 2011). However, the negative net charge of SPC at pH 8.0 could contribute to a higher FRAP antioxidant capacity due to a positive interaction between the protein and ferric ions. The FRAP value obtained for pH 8.0 was higher than that of Chatsuwan et al., (Chatsuwan et al., 2018) who reported FRAP values of 54.20 ± 0.13 μg TE g^{-1} protein in an aqueous protein extract of *Bombyx mori.*

3.2. Interfacial characterisation

3.2.1. Determination of surface tension at equilibrium

Protein saturation of the SPC protein supernatants (obtained at pH 2.0 and 8.0) at the A/W interface was determined using a Wilhelmy plate connected to a tensiometer. Fig. 3A shows

the surface tension obtained as a function of protein concentration after complete protein adsorption (24 h) at pH 2.0 and 8.0. Increasing concentrations of the SPC protein system resulted in a decrease in surface tension prior to A/W interface saturation. This result was previously related to an increase in protein concentration at the A/W interface, leading to lower surface tension values (Eric Dickinson, 1998). However, once the interface was saturated, any further increases in protein concentration did not lead to a decrease in surface tension (Tie, Calonder, & Van Tassel, 2003). The protein concentration at which the interface is saturated is defined as the adsorption efficiency (AE) whereas the minimum interfacial tension at the plateau is defined as the surface activity (SA). According to the results obtained herein, the AE of the SPC protein system at the A/W interface was 2 wt. % (Fig. 3). This was higher than the saturation concentration found for other highly soluble model proteins such as BSA, β lactoglobulin or casein (Cascão Pereira et al., 2003; Cicuta, 2007). However, the SPC protein system exhibited a similar saturation concentration to plant proteins such chickpea (Felix, Romero, Sanchez, & Guerrero, 2019), faba (Felix, Romero, Carrera-Sanchez, & Guerrero, 2019) and soy bean (Martínez, Sánchez, Patino, & Pilosof, 2009). The SPC protein system evaluated in this study reached an SA value of c.a. 42 mN/m. This interfacial tension value was lower than a soy protein hydrolysate (Patino et al., 2007) and similar to soy globulin in the absence of sucrose (Ruiz-Henestrosa, Carrera-Sanchez, & Rodriguez-Patino, 2008b).

Fig. 3B shows the evolution of surface tension during protein adsorption until reaching a quasi-equilibrium (t = 180 min) at both pH values (2.0 and 8.0) when analysed at the protein saturation concentration (2 wt.%). The evolution of surface tension was characterised by an initial rapid decrease, followed by a slower decrease until reaching a quasi-constant value (σ_{eq}). This near constant value is known as pseudo-equilibrium state of the protein adsorbed at the A/W interface. ~~The pattern of the decrease in surface tension has been related with different phenomena.~~ Although there is no general model which explains the complete behaviour of

proteins at interfaces, the first step (fast kinetics) has been previously related to migration of the proteins from the bulk towards the A/W interface (protein diffusion) (Baldursdottir, Fullerton, Nielsen, & Jorgensen, 2010). The subsequent stage characterised by a slower decrease in interfacial tension has been related to the penetration, unfolding and rearrangement of proteins at the interface (Beverung, Radke, & Blanch, 1999; Pérez, Sánchez, Pilosof, & Rodríguez, 2009; Rodriguez Patino, Rodriguez Nino, & Sanchez, 1999). The results in the inset in Figure 3B indicate that protein diffusion from the bulk to the interface occurred faster at pH 8.0 (higher k_D^*). However, protein penetration and rearrangement was faster at pH 2.0 (higher k_A). This smaller k_A at pH 2.0 can justify that the interfacial tension observed at pH 2.0 by droplet tensiometer was smaller at pH 2.0 (after 3 h protein adsorption), however the interfacial tension at pH 2.0 and 8.0 were similar by Wilhelmy plate (after 24 h protein adsorption). Results from electrophoresis (Fig. 2) indicated that bigger protein sizes were found at pH 2.0. According to Ward and Tordai equation (1946) molecular weight is inversely proportional to protein diffusion. In both cases, different kinetics of absorption and rearrangement were observed at pH 2.0 and 8.0. However, both samples reached similar interfacial tension values after 24h protein adsorption. Nevertheless, these values (15 – 50 mN/m) were similar to the final surface tension values obtained for plant proteins such as those from faba bean, pea, chickpea, lentil and soy (Karaca, Low, & Nickerson, 2011).

3.2.2. Interfacial rheology measurements

Further dilatational and interfacial shear experiments were carried out to elucidate the interfacial structure of these systems in order to understand the behaviour of the interfacial films.

a) Linear viscoelastic dilatational measurements

The viscoelastic properties of SPC protein adsorbed at the A/W interface are shown before reaching the quasi-equilibrium state (t < 180 min, Fig 4A) and after reaching the quasi-

equilibrium-state (t > 180 min, Fig 4B) at pH 2.0 and 8.0. Similar responses were obtained during protein adsorption at the A/W interface, regardless of the pH value. The response was characterised by an initial rapid increase in the elastic modulus (E'_s), followed by a tendency to reach a plateau. Moreover, the viscous modulus (E''_s) decreased until reaching a nearly constant value. This rheological response has been previously reported in milk and crayfish proteins which has been related to the development of a protein film at the A/W interface (E Dickinson, 2003; Felix, Romero, & Guerrero, 2017). However, although the formation of these protein films occurred in a similar manner, the dynamics observed were different. In this sense, protein adsorption at pH 8.0 seemed to be faster, since it was characterised by a smaller evolution of the dilatational moduli during the time period studied. These results are in agreement with those shown in Figure 3B where the kinetics of protein absorption were faster at pH 8.0. This different evolution may be related with the smaller protein sizes found at pH 8.0, which influences in the adsorption stages as mentioned earlier (diffusion, penetration, adsorption, rearrangements and relaxation). A phenomena which may explain why the use of protein hydrolysates also reduce hydrophobic interactions at the interface (Patino et al., 2007). The results shown in Fig. 4A confirms that protein diffusion and adsorption at the A/W interface was faster at pH 8.0 than at pH 2.0. However, the exact processes occurring during SPC protein adsorption at the A/W interface would require further investigation. According to the estimated kinetic parameters, protein adsorption occurred much faster at pH 8.0 (higher k_D^*), although protein penetration and rearrangement occurred to a greater extent at pH 2.0 (higher k_A). Consequently, higher dilatational viscoelastic moduli were obtained at pH 2.0. These results must be related to the higher molecular sizes found at pH 2.0 which provided the stronger surface coverage observed in dilatational measurements. In this sense, relaxation mechanisms such as diffusion exchange within the bulk or conformational changes in the monolayer formed,

which are related to the protein network developed, seemed to be more limited at pH 8.0 resulting therefore, in less extensive protein-protein interactions (Cascão Pereira et al., 2003). Fig. 4B shows the mechanical spectra obtained by means of frequency sweep tests (from 0.0075 to 0.1 Hz) for the SPC protein film formed at the A/W interface on reaching the pseudo-equilibrium state (t > 180 min). These spectra confirmed the formation of an interfacial protein film which had a gel-like behaviour, since the E'_s values were always greater than E''_s (Felix, Romero, Sanchez, et al., 2019). The elastic modulus showed a typical frequency-dependence for the two pH values analysed ($G' \sim \omega^n$) regardless of the pH. However, the E'_s values were higher for the SPC protein adsorbed at the A/W interface at pH 2.0 than the corresponding values at pH 8.0, suggesting that the protein molecules adsorbed at acidic pH developed more elastic interfacial films. This behaviour was also found for other proteins adsorbed at O/W interfaces such as potato (Romero et al., 2011), rice (Romero et al., 2012), crayfish (Felix, Romero, Vermant, & Guerrero, 2016), chickpea (Felix, Romero, Sanchez, et al., 2019) and faba bean (Felix, Romero, Carrera-Sanchez, et al., 2019).

b) Linear viscoelastic interfacial shear measurements

Fig. 5 shows the viscoelastic properties obtained from small amplitude oscillatory shear (i-SAOS) measurements for SPC protein adsorbed at the A/W interface as a function of protein adsorption (t < 180 min, Fig 5A) and after reaching the quasi-equilibrium-state (t > 180 min, Fig 5B) at pH 2.0 and 8.0. Fig. 5A indicates that although the final values for the interfacial viscoelastic moduli were similar regardless of the pH value studied, their evolution was different depending on the pH value analysed. In this sense, the interfacial film is developed faster at pH 8.0 than at pH 2.0 (which agree with the smaller molecular sizes observed at pH 8.0 by electrophoresis). This behaviour was also observed in the dilatational measurements (Fig. 4), where that the quasi-equilibrium state was reached much faster at pH 8.0. The i-SAOS response obtained for the A/W interface at pH 2.0 was characterised by a decrease until a

406 constant value was reached. Since the viscoelastic response obtained by means of interfacial
407 shear measurements had been attributed to cohesive interactions with neighbouring
408 molecules (Narsimhan, 2016), these results suggest that after initial protein adsorption (protein
409 diffusion was not observed by i-SAOS measurements since the initial data point was acquired
410 after 10 min protein adsorption) the interfacial film changed, resulting in no significant
411 differences at the end of the protein adsorption period. Moreover, this result confirms that the
412 development of the interfacial layers at pH 2.0 was slower than at pH 8.0, which can be related
413 to the above-mentioned higher molecular sizes at pH 2.0.
414 Fig. 5B shows the mechanical spectra obtained by means of i-SAOS measurements (from
415 0.0075 to 0.3 Hz) for the SPC protein film formed at the A/W interface after reaching the quasi-
416 equilibrium state (t > 180 min). This spectra confirmed the formation of a protein film which
417 had a gel-like behaviour, since G'_s was larger than G''_s (Felix, Romero, Sanchez, et al., 2019).
418 Similar to dilatational measurements, although $\tan \delta_S$ was < 1 ($G'_s > G''_s$), where the elastic
419 modulus showed a more marked frequency dependence~~, which was more marked~~ at pH 8.0. In
420 order to quantify this frequency dependency, the slope of the viscous moduli (G') was
421 calculated, leading to the following values: 0.03 ± 0.01 and 0.32 ± 0.05, for pH 2.0 and 8.0,
422 respectively. This result indicated that the gel-like behaviour of the interfacial film at pH 8.0
423 was weaker than that observed at pH 2.0, which was in agreement with previous dilatational
424 measurements. Thus, the mechanical spectra obtained for pH 8.0 indicated that there is a lower
425 extent of protein-protein interactions at pH 8.0 since at this pH there is a higher frequency
426 dependence (although it can be noticed that the differences are not strongly market, and the
427 rheometer is close to its confidence limit)~~.~~
428 *Foaming properties*
429 Fig. 6 shows the liquid volume in the foam as a function of time in foams generated with the
430 SPC protein system at 20 °C and pH 2.0 (A) and pH 8.0 (B). The foaming properties of the SPC

protein strongly depended on the pH value. The maximum liquid volume in the foam was 12 and 2.5 cm^3 at the end of the foaming step (by bubbling N_2) for sample at pH 2.0 and 8.0, respectively. Thus, according to the procedure explained in section 2.6, only the foam at pH 2.0 reached the target volume (12 cm^3) during the experiment carried out. Consequently, foam stability at pH 8.0 was not possible to measure. This different foaming capacity was also reflected in foam stability, where the $t_{1/2}$ for the foam at pH 2.0 was 265 s and no $t_{1/2}$ value could be calculated for the foam at pH 8.0 since the destabilization phenomena were faster than foam generation. These results indicated that the foaming capacity of SPC at pH 2.0 was higher than at pH 8.0. Foaming capacity and stability may be correlated with the interfacial properties previously described. Dilatational and interfacial shear rheology indicated that the interfacial film formed at pH 2.0 was more elastic. However, when SPC was adjusted to pH 8.0, interfacial characterisation suggested that the interface formed was weaker (although interfacial shear measurements did not show marked differences). Consequently, the rheological response obtained in dilatational measurements showed higher viscoelastic moduli, at the same time as the interfacial shear measurements indicated that the interface was also more elastic at pH 2.0. Table 3 compares different parameters for foam formation and stability obtained using the same protocol and equipment for SPC protein and three other protein systems previously reported (sunflower protein isolate, sucrose/soy globulin mixtures and sodium caseinate). The OFC obtained was 0.82 ± 0.03, which is similar to previous values obtained for sodium caseinate/protein systems (Sánchez & Patino, 2005), hydrolysed sunflower protein concentrate (Martinez, Carrera-Sanchez, Ruiz-Henestrosa, Rodríguez-Patino, & Pilosof, 2007) and soy globulin/sucrose systems (Pizones Ruiz-Henestrosa et al., 2008b). This confirms that the SPC protein system was of potential interest for the food industry as foaming agent in the formation of a wide range of acid foams. According to the FC, MD and CF (%) parameters show in Table 3 (1.03 ± 0.02, 0,10 ± 0.01 and 28.2 ± 0.1, respectively), SPC proteins had a good foaming

456 capacity leading to small and dense bubbles. These values were comparable with those obtained
457 for other protein systems from sunflower, sodium caseinate and soy globulin (Patino et al.,
458 2007; Ruiz-Henestrosa et al., 2008b; Sánchez & Patino, 2005).
459 Moreover, Table 3 also shows the mean $t_{1/2}$ of these systems. The foam stability of the SPC-
460 based foam was shorter than the above-mentioned protein-based foams stabilized by sunflower
461 protein isolate and sucrose/soy globulin (Patino et al., 2007; Pizones Ruiz-Henestrosa et al.,
462 2008b). However, Pizones et al. (2008b) reported a $t_{1/2}$ of 250s for 7S globulin which was
463 similar to the value obtained for the foam stabilized by the SPC protein system herein.
464 Eventually, comparing results from interfacial measurements and foaming capacity at pH 2.0
465 and pH 8.0, it could be concluded that the foaming capacity of SPC was determined by the
466 dynamics of the interface as in the sunflower protein system (Patino et al., 2007).
467 Fig. 7 shows images of the bubbles formed, as well as their bubble size distribution, after N_2
468 gas sparking as a function of time at pH 2.0 (results at pH 8.0 were not available since the foam
469 did not reach the CCD camera height). Two different bubble sizes were formed, where bigger
470 bubbles appear to increase their size at the expense of small bobbles as time progressed. This
471 destabilization phenomenon known as Ostwald ripening was previously observed for other
472 foam systems (Murray & Ettelaie, 2004). This phenomenon was also observed in the bubble
473 size distribution since the main peak suffered a displacement towards higher values (decreasing
474 the number of small bubbles). Therefore, the camera images confirmed the suitability of this
475 protein to form and stabilize A/W interfaces, however, further studies are required in order to
476 improve the stability of the foam generated at pH 2.0.

477 **4. Concluding remarks**

478 The results obtained indicate that silkworm pupae, which is a by-product from silk industry,
479 can be used to obtain a protein concentrate. The SPC obtained exhibited functional properties

suitable for the development of multiphasic food products such as foams with antioxidant properties. The SPC used had a protein content of 71.0 ± 1.4 wt.%, it had a moderate solubility which ranged from 31.6 ± 1.2 % (pH 5.0) to 60.1 ± 2.5 % (pH 10.0). Two pH values were selected for further characterisation: pH 2.0 and 8.0. Antioxidant activity characterisation indicated that these protein systems exhibited antioxidant activity, which depended on pH value, with the best results being obtained at pH 8.0 (1826.0 ± 131.9 and 168.0 ± 3.0 for the FRAP and ORAC assays, respectively). Interfacial characterisation revealed similar interfacial tension values after protein adsorption at equilibrium. However, the kinetics of SPC protein adsorption depended on pH since the interfacial tension was lower at pH 8.0 than at pH 2.0 after 180 min protein adsorption. This result was related to the occurrence of several mechanisms (protein relaxation, protein rearrangement and multilayer formation) which may stabilize the interface in the longer timescale. The rheological characterisation of the A/W interface (as assessed by means of droplet measurements and i-SAOS) supported the previous results, since a slower evolution was observed at pH 2.0 than at pH 8.0. Furthermore, the interfacial properties were correlated with the foaming capacity and stability of the protein system. In this sense, the foaming capacity was higher at pH 2.0, leading to higher foam expansion (and consequently higher foam height). Eventually, the results indicated that interfacial measurements were useful to predict the final interfacial properties of dispersed protein systems.

5. Acknowledgments

The authors also acknowledge University of Seville for the VPPI-US grant (Ref.-II.5) to Manuel Felix. Authors also acknowledge the financial support of the Spanish Government "Ministerio de Ciencia, Innovación y Universidades" by the grant Ref. RTI2018-097100-B-C21, MICINN/FEDER, UE. The authors acknowledge funding to Maria Cermeño under the National Development Plan 2007–2013, through the Food Institutional Research Measure

(FIRM), administered by the Department of Agriculture, Food and Marine, Ireland under grant issue 15/F/647.

6. References

A.O.A.C. (2000). *Official Methods of Analysis*. (W. Horwitz, Ed.) (11th ed.). Wisconsin: Association of Official Analytical Chemist.

Baldursdottir, S. G., Fullerton, M. S., Nielsen, S. H., & Jorgensen, L. (2010). Adsorption of proteins at the oil/water interface—Observation of protein adsorption by interfacial shear stress measurements. *Colloids and Surfaces B: Biointerfaces*, *79*(1), 41–46. https://doi.org/http://dx.doi.org/10.1016/j.colsurfb.2010.03.020

Beverung, C. J., Radke, C. J., & Blanch, H. W. (1999). Protein adsorption at the oil/water interface: characterization of adsorption kinetics by dynamic interfacial tension measurements. *Biophysical Chemistry*, *81*(1), 59–80. https://doi.org/10.1016/s0301-4622(99)00082-4

Boland, M. J., Rae, A. N., Vereijken, J. M., Meuwissen, M. P. M., Fischer, A. R. H., van Boekel, M. A. J. S., … Hendriks, W. H. (2013). The future supply of animal-derived protein for human consumption. *Trends in Food Science & Technology*, *29*(1), 62–73. https://doi.org/http://dx.doi.org/10.1016/j.tifs.2012.07.002

Boye, J., Zare, F., & Pletch, A. (2010). Pulse proteins: Processing, characterization, functional properties and applications in food and feed. *Food Research International*, *43*(2), 414–431. https://doi.org/https://doi.org/10.1016/j.foodres.2009.09.003

Bruinsma, J., & others. (2009). The resource outlook to 2050: By how much do land, water and crop yields need to increase by 2050. In *Expert meeting on how to feed the world in* (Vol. 2050, pp. 24–26).

527 Caro, A. L., Niño, M. R. R., Sánchez, C. C., Gunning, A. P., Mackie, A. R., & Patino, J. M.
528 R. (2005). Displacement of β-casein from the air-water interface by phospholipids. In
529 Eric Dickinson (Ed.), *Food Colloids: Interactions{,} Microstructure and Processing* (pp.
530 160–176). The Royal Society of Chemistry. https://doi.org/10.1039/9781847552389-
531 00160

532 Cascão Pereira, L. G., Théodoly, O., Blanch, H. W., Radke, C. J., Pereira, L. G. C., Theodoly,
533 O., … Radke, C. J. (2003). Dilatational Rheology of BSA Conformers at the Air/Water
534 Interface. *Langmuir*, *19*(6), 2349–2356. https://doi.org/10.1021/la020720e

535 Castellani, O., Al-Assaf, S., Axelos, M., Phillips, G. O., & Anton, M. (2010). Hydrocolloids
536 with emulsifying capacity. Part 2-Adsorption properties at the n-hexadecane-Water
537 interface. *Food Hydrocolloids*, *24*(2–3), 121–130.
538 https://doi.org/10.1016/j.foodhyd.2009.07.006

539 Cermeño, M., FitzGerald, R. J., & O'Brien, N. M. (2016). In vitro antioxidant and
540 immunomodulatory activity of transglutaminase-treated sodium caseinate hydrolysates.
541 *International Dairy Journal*, *63*(Supplement C), 107–114.
542 https://doi.org/https://doi.org/10.1016/j.idairyj.2016.08.007

543 Chang, C., Tu, S., Ghosh, S., & Nickerson, M. T. (2015). Effect of pH on the inter-
544 relationships between the physicochemical, interfacial and emulsifying properties for
545 pea, soy, lentil and canola protein isolates. *Food Research International*, *77*, *Part 3*,
546 360–367. https://doi.org/http://dx.doi.org/10.1016/j.foodres.2015.08.012

547 Chatsuwan, N., Puechkamut, Y., & Pinsirodom, P. (2018). Characterization , Functionality
548 and Antioxidant Activity of Water-Soluble Proteins Extracted from Bombyx mori Linn .,
549 *18*(2), 83–96. https://doi.org/10.14456/cast.2018.4

Cicuta, P. (2007). Compression and shear surface rheology in spread layers of β-casein and β-lactoglobulin. *Journal of Colloid and Interface Science*, *308*(1), 93–99. https://doi.org/https://doi.org/10.1016/j.jcis.2006.12.056

David-Birman, T., Moshe, H., & Lesmes, U. (2019). Impact of thermal processing on physicochemical properties of silk moth pupae (Bombyx mori) flour and in-vitro gastrointestinal proteolysis in adults and seniors. *Food Research International*, *123*, 11–19. https://doi.org/https://doi.org/10.1016/j.foodres.2019.04.042

Dickinson, E. (2003). Interfacial, Emulsifying and Foaming Properties of Milk Proteins. In P. F. Fox & P. L. H. McSweeney (Eds.), *Advanced Dairy Chemistry---1 Proteins: Part A / Part B* (pp. 1229–1260). Boston, MA: Springer US. https://doi.org/10.1007/978-1-4419-8602-3_33

Dickinson, Eric. (1998). Proteins at interfaces and in emulsions Stability, rheology and interactions. *J. Chem. Soc., Faraday Trans.*, *94*(12), 1657–1669. https://doi.org/10.1039/A801167B

Felix, M., Romero, A., & Guerrero, A. (2017). Viscoelastic properties, microstructure and stability of high-oleic O/W emulsions stabilised by crayfish protein concentrate and xanthan gum. *Food Hydrocolloids*, *64*, 9–17. https://doi.org/10.1016/j.foodhyd.2016.10.028

Felix, M., Romero, A., Vermant, J., & Guerrero, A. (2016). Interfacial properties of highly soluble crayfish protein derivatives. *Colloids and Surfaces A: Physicochemical and Engineering Aspects*, *499*. https://doi.org/10.1016/j.colsurfa.2016.03.037

Felix, Manuel, Romero, A., Carrera-Sanchez, C., & Guerrero, A. (2019). Assessment of interfacial viscoelastic properties of Faba bean (Vicia faba) protein-adsorbed O/W layers

573 as a function of pH. *Food Hydrocolloids*, *90*, 353–359.
574 https://doi.org/https://doi.org/10.1016/j.foodhyd.2018.12.036

575 Felix, Manuel, Romero, A., Sanchez, C. C., & Guerrero, A. (2019). Modelling the non-linear
576 interfacial shear rheology behaviour of chickpea protein-adsorbed complex oil/water
577 layers. *Applied Surface Science*, *469*, 792–803.
578 https://doi.org/https://doi.org/10.1016/j.apsusc.2018.11.074

579 Ferry, J. D. (1980). *Viscoelastic properties of polymers*. Wiley.

580 Jena, K., Kar, P. K., Kausar, Z., & Babu, C. S. (2013). Effects of temperature on modulation
581 of oxidative stress and antioxidant defenses in testes of tropical tasar silkworm
582 Antheraea mylitta. *Journal of Thermal Biology*, *38*(4), 199–204.
583 https://doi.org/https://doi.org/10.1016/j.jtherbio.2013.02.008

584 Karaca, A. C., Low, N., & Nickerson, M. (2011). Emulsifying properties of chickpea, faba
585 bean, lentil and pea proteins produced by isoelectric precipitation and salt extraction.
586 *Food Research International*, *44*(9), 2742–2750.
587 https://doi.org/http://dx.doi.org/10.1016/j.foodres.2011.06.012

588 Kim, H.-W., Setyabrata, D., Lee, Y. J., Jones, O. G., & Kim, Y. H. B. (2016). Pre-treated
589 mealworm larvae and silkworm pupae as a novel protein ingredient in emulsion
590 sausages. *Innovative Food Science & Emerging Technologies*, *38*, 116–123.
591 https://doi.org/https://doi.org/10.1016/j.ifset.2016.09.023

592 Koeppel, A., & Holland, C. (2017). Progress and Trends in Artificial Silk Spinning: A
593 Systematic Review. *ACS Biomaterials Science & Engineering*, *3*(3), 226–237.
594 https://doi.org/10.1021/acsbiomaterials.6b00669

595 Kumar, D., Dev, P., & Kumar, R. V. (2015). Biomedical Applications of Silkworm Pupae

596 Proteins (pp. 41–49). Springer, New Delhi. https://doi.org/10.1007/978-81-322-2491-4_3

597 Lieselot Vercruysse, Guy Smagghe, G., Herregods, C., & Van, J. (2005). ACE Inhibitory
598 Activity in Enzymatic Hydrolysates of Insect Protein.
599 https://doi.org/10.1021/JF050337Q

600 Liu, Y., Wan, S., Liu, J., Zou, Y., & Liao, S. (2017). Antioxidant Activity and Stability Study
601 of Peptides from Enzymatically Hydrolyzed Male Silkmoth. *Journal of Food Processing*
602 *and Preservation*, *41*(1), e13081. https://doi.org/10.1111/jfpp.13081

603 Lowry, O. H. (1951). The folin by oliver. *Analytical Biochemistry*, *217*(2), 220–230.
604 https://doi.org/10.1016/0304-3894(92)87011-4

605 Mahendran, B., Ghosh, S. K., & Kundu, S. C. (2006). Molecular phylogeny of silk producing
606 insects based on internal transcribed spacer DNA1. *Journal of Biochemistry and*
607 *Molecular Biology*, *39*(5), 522–529.

608 Marathe, S. A., Rajalakshmi, V., Jamdar, S. N., & Sharma, A. (2011). Comparative study on
609 antioxidant activity of different varieties of commonly consumed legumes in India. *Food*
610 *and Chemical Toxicology*, *49*(9), 2005–2012.
611 https://doi.org/http://dx.doi.org/10.1016/j.fct.2011.04.039

612 Markwell, M. A. K., Haas, S. M., Bieber, L. L., & Tolbert, N. E. (1978). Modification of
613 Lowry procedure to simplify protein determination in membrane and lipoprotein
614 samples. *Analytical Biochemistry*, *87*(1), 206–210. https://doi.org/10.1016/0003-
615 2697(78)90586-9

616 Martinez, K. D., Carrera Sanchez, C., Pizones Ruiz-Henestrosa, V., Rodríguez Patino, J. M.,
617 & Pilosof, A. M. R. (2007). Soy protein–polysaccharides interactions at the air–water
618 interface. *Food Hydrocolloids*, *21*(5), 804–812.

https://doi.org/https://doi.org/10.1016/j.foodhyd.2006.11.005

Martínez, K. D., Sánchez, C. C., Patino, J. M. R., & Pilosof, A. M. R. (2009). Interfacial and foaming properties of soy protein and their hydrolysates. *Food Hydrocolloids*, *23*(8), 2149–2157. https://doi.org/https://doi.org/10.1016/j.foodhyd.2009.03.015

Martinez, M. J., Carrera Sánchez, C., Rodríguez Patino, J. M., & Pilosof, A. M. R. (2012). Interactions between β-lactoglobulin and casein glycomacropeptide on foaming. *Colloids and Surfaces B: Biointerfaces*, *89*, 234–241. https://doi.org/10.1016/j.colsurfb.2011.09.022

McClements, D. J. (2015). Food Emulsions. *Food Emulsions Principles, Practices, and Techniques*. https://doi.org/10.1201/b18868

Multari, S., Stewart, D., & Russell, W. R. (2015). Potential of Fava Bean as Future Protein Supply to Partially Replace Meat Intake in the Human Diet. *Comprehensive Reviews in Food Science and Food Safety*, *14*(5), 511–522. https://doi.org/10.1111/1541-4337.12146

Murray, B. S., & Ettelaie, R. (2004). Foam stability: Proteins and nanoparticles. *Current Opinion in Colloid and Interface Science*. https://doi.org/10.1016/j.cocis.2004.09.004

Narsimhan, G. (2016). Characterization of Interfacial Rheology of Protein-Stabilized Air--Liquid Interfaces. *Food Engineering Reviews*, *8*(3), 367–392. https://doi.org/10.1007/s12393-015-9133-z

Noskov, B. A., Mikhailovskaya, A. A., Lin, S. Y., Loglio, G., & Miller, R. (2010). Bovine Serum Albumin Unfolding at the Air/Water Interface as Studied by Dilational Surface Rheology. *Langmuir*, *26*(22), 17225–17231. https://doi.org/10.1021/la103360h

641 Oonincx, D. G. A. B., van Itterbeeck, J., Heetkamp, M. J. W., van den Brand, H., van Loon, J.
642 J. A., & van Huis, A. (2011). An Exploration on Greenhouse Gas and Ammonia
643 Production by Insect Species Suitable for Animal or Human Consumption. *PLOS ONE*,
644 *5*(12), 1–7. https://doi.org/10.1371/journal.pone.0014445

645 Patino, J M R, Conde, J. M., Linares, H. M., Jimenez, J. J. P., Sanchez, C. C., Pizones, V., &
646 Rodriguez, F. M. (2007). Interfacial and foaming properties of enzyme-induced
647 hydrolysis of sunflower protein isolate. *Food Hydrocolloids*, *21*(5–6), 782–793.
648 https://doi.org/10.1016/j.foodhyd.2006.09.002

649 Patino, Juan M.Rodríguez, Niño, R. R., & Gómez, J. M. Á. (1997). Interfacial and foaming
650 characteristics of protein—lipid systems. *Food Hydrocolloids*, *11*(1), 49–58.
651 https://doi.org/https://doi.org/10.1016/S0268-005X(97)80010-0

652 Perez, A. A., Carrera, C. R., Sanchez, C. C., Santiago, L. G., & Patino, J. M. R. (2009).
653 Interfacial dynamic properties of whey protein concentrate/polysaccharide mixtures at
654 neutral pH. *Food Hydrocolloids*, *23*(5), 1253–1262.
655 https://doi.org/10.1016/j.foodhyd.2008.08.013

656 Pérez, O., Sánchez, C., Pilosof, A., & Rodríguez, J. M. (2009). chang 2015. *Journal of*
657 *Colloid and Interface Science*, *336*(2), 485–496.
658 https://doi.org/10.1016/j.jcis.2009.04.011

659 Pizones Ruiz-Henestrosa, V., Carrera Sanchez, C., & Rodriguez Patino, J. M. (2008a).
660 Adsorption and foaming characteristics of soy globulins and tween 20 mixed systems.
661 *Industrial & Engineering Chemistry Research*, *47*(9), 2876–2885.
662 https://doi.org/10.1021/ie071518f

663 Pizones Ruiz-Henestrosa, V., Carrera Sanchez, C., & Rodriguez Patino, J. M. (2008b). Effect

of sucrose on functional properties of soy globulins: Adsorption and foam characteristics. *Journal of Agricultural and Food Chemistry*, *56*(7), 2512–2521. https://doi.org/10.1021/jf0731245

Prasad, M. D., Muthulakshmi, M., Madhu, M., Archak, S., Mita, K., & Nagaraju, J. (2005). Survey and analysis of microsatellites in the silkworm, Bombyx mori: frequency, distribution, mutations, marker potential and their conservation in heterologous species. *Genetics*, *169*(1), 197–214. https://doi.org/10.1534/genetics.104.031005

Reddy, K. D., Abraham, E. G., & Nagaraju, J. (1999). Microsatellites in the silkworm, Bombyx mori: abundance, polymorphism, and strain characterization. *Genome*, *42*(6), 1057–1065.

Rodríguez Patino, J. M., Carrera Sánchez, C., Molina Ortiz, S. E., Rodríguez Niño, M. R., & Añón, M. C. (2004). Adsorption of Soy Globulin Films at the Air−Water Interface. *Industrial & Engineering Chemistry Research*, *43*(7), 1681–1689. https://doi.org/10.1021/ie0302443

Rodriguez Patino, J. M., Rodriguez Nino, M. R., & Sanchez, C. C. (1999). Adsorption of whey protein isolate at the oil-water interface as a function of processing conditions: a rheokinetic study. *Journal of Agricultural and Food Chemistry*, *47*(6), 2241–2248. https://doi.org/10.1021/jf981119i

Romero, A., Beaumal, V., David-Briand, E., Cordobes, F., Guerrero, A., & Anton, M. (2011). Interfacial and Oil/Water Emulsions Characterization of Potato Protein Isolates. *Journal of Agricultural and Food Chemistry*, *59*(17), 9466–9474. https://doi.org/10.1021/jf2019853

Romero, A., Beaumal, V., David-Briand, E., Cordobes, F., Guerrero, A., & Anton, M. (2012).

687 Interfacial and emulsifying behaviour of rice protein concentrate. *Food Hydrocolloids*,
688 *29*(1), 1–8. https://doi.org/10.1016/j.foodhyd.2012.01.013

689 Sánchez, C. C., & Patino, J. M. R. (2005). Interfacial, foaming and emulsifying characteristics
690 of sodium caseinate as influenced by protein concentration in solution. *Food*
691 *Hydrocolloids*, *19*(3), 407–416.
692 https://doi.org/http://dx.doi.org/10.1016/j.foodhyd.2004.10.007

693 Schwenzfeier, A., Lech, F., Wierenga, P. A., Eppink, M. H. M., & Gruppen, H. (2013). Foam
694 properties of algae soluble protein isolate: Effect of pH and ionic strength. *Food*
695 *Hydrocolloids*, *33*(1), 111–117. https://doi.org/10.1016/j.foodhyd.2013.03.002

696 Sjödin, A. M. (2018). Safety of Whey basic protein isolates as a novel food pursuant to
697 Regulation (EU) 2015/2283: Scientific Opinion. *EFS a Journal*, *16*(7).

698 Spada, J. C., Marczak, L. D. F., Tessaro, I. C., & Cardozo, N. S. M. (2015). Interactions
699 between soy protein from water-soluble soy extract and polysaccharides in solutions with
700 polydextrose. *Carbohydrate Polymers*, *134*, 119–127.
701 https://doi.org/https://doi.org/10.1016/j.carbpol.2015.07.075

702 Takechi, T., Wada, R., Fukuda, T., Harada, K., & Takamura, H. (2014). Antioxidant activities
703 of two sericin proteins extracted from cocoon of silkworm (Bombyx mori) measured by
704 DPPH, chemiluminescence, ORAC and ESR methods. *Biomedical Reports*, *2*(3), 364–
705 369.

706 Tie, Y., Calonder, C., & Van Tassel, P. R. (2003). Protein adsorption: Kinetics and history
707 dependence. *Journal of Colloid and Interface Science*, *268*(1), 1–11.
708 https://doi.org/10.1016/s0021-9797(03)00516-2

709 Tomotake, H., Katagiri, M., & Yamato, M. (2010). Silkworm Pupae (Bombyx mori) Are New

710 Sources of High Quality Protein and Lipid. *Journal of Nutritional Science and*
711 *Vitaminology*, *56*(6), 446–448. https://doi.org/10.3177/jnsv.56.446

712 Vandebril, S., Franck, A., Fuller, G. G., Moldenaers, P., & Vermant, J. (2010). A double wall-
713 ring geometry for interfacial shear rheometry. *Rheologica Acta*, *49*(2), 131–144.
714 https://doi.org/10.1007/s00397-009-0407-3

715 Wan, Z., Yang, X., & Sagis, L. M. C. (2016). Nonlinear Surface Dilatational Rheology and
716 Foaming Behavior of Protein and Protein Fibrillar Aggregates in the Presence of Natural
717 Surfactant. *Langmuir*, *32*(15), 3679–3690. https://doi.org/10.1021/acs.langmuir.6b00446

718 Wang, W., Wang, N., Zhou, Y., Zhang, Y., Xu, L., Xu, J., … He, G. (2011). Isolation of a
719 novel peptide from silkworm pupae protein components and interaction characteristics to
720 angiotensin I-converting enzyme. *European Food Research and Technology*, *232*(1), 29–
721 38. https://doi.org/10.1007/s00217-010-1358-8

722 Ward, A. F. H., & Tordai, L. (1946). Time-dependence of boundary tensions of solutions. 1.
723 The role of diffusion in time-effects. *Journal of Chemical Physics*, *14*(7), 453–461.
724 https://doi.org/10.1063/1.1724167

725 Wimer, L. T. (1969). A comparison of the carbohydrate composition of the hemolymph and
726 fat body of Phormia regina during larval development. *Comparative Biochemistry and*
727 *Physiology*, *29*(3), 1055–1062. https://doi.org/https://doi.org/10.1016/0010-
728 406X(69)91008-1

729 Wu, X. L., Zhao, D., & Yang, S. T. (2011). Impact of solution chemistry conditions on the
730 sorption behavior of Cu(II) on Lin'an montmorillonite. *Desalination*, *269*(1), 84–91.
731 https://doi.org/http://dx.doi.org/10.1016/j.desal.2010.10.046

732 Xia, L., Ng, T. B., Fang, E. F., & Wong, J. H. (2013). Bioactive Constituents of the Silk

733 Worm Bombyx mori. In *Antitumor Potential and other Emerging Medicinal Properties*
734 *of Natural Compounds* (pp. 335–344). Dordrecht: Springer Netherlands.
735 https://doi.org/10.1007/978-94-007-6214-5_22

736 Zhai, F.-H., Wang, Q., & Han, J.-R. (2015). Nutritional components and antioxidant
737 properties of seven kinds of cereals fermented by the basidiomycete Agaricus blazei.
738 *Journal of Cereal Science*, *65*, 202–208.
739 https://doi.org/http://dx.doi.org/10.1016/j.jcs.2015.07.010

740

741

Table 1

Table 1: Proximate composition of the silkworm protein concentrate (SPC) before and after defatting.

	Before defatting	**After defatting**
Component	**% (w/w)**	**% (w/w)**
Protein	50.5 ± 1.0	71.0 ± 1.4
Lipid	28.9 ± 0.2	< 0.2
Carbohydrates*	5.1	7.2
Moisture	8.9 ± 0.1	12.5 ± 1.4
Ash	6.6 ± 0.8	9.3 ± 1.1

*Determined by difference

Table 2

Table 2: Ferric-reducing antioxidant power (FRAP) and oxygen radical absorbance capacity (ORAC) antioxidant activity of the protein concentrate obtained from the silkworm pupae (SPC) solubilized at pH 2.0 and 8.0. Values represent the mean of three independent replicates (n=3). Different letters within a column indicate significant differences ($p < 0.05$).

	Antioxidant activity (µmols Eq. Trolox·g^{-1} protein)	
pH value	**FRAP**	**ORAC**
pH 2.0	1659.2 ± 46.8^{a}	43.5 ± 8.1^{b}
pH 8.0	1826.0 ± 131.9^{a}	168.0 ± 3.0^{a}

Table 3

Table 3: Comparison of parameters obtained during foam formation and breakdown at pH 2.0 with other protein systems as previously reported in the literature using a FOAMSCAM device under the same operation conditions.

	Protein system			
Parameter	**Silkworm protein concentrate (SPC)**	**Sunflower**	**Sucrose/Soy Globulin**	**Sodium caseinate**
OFC (mL/s)	0.82 ± 0.03	0.8	0.8	1
FC	1.03 ± 0.02	1	0.8	0.8
CF (%)	28.2 ± 0.1	40	-	32
MD	0.10 ± 0.01	0.12	-	0.12
$t_{1/2}$ (s)	105 ± 3	400	250	-
Reference	*Present study*	*Patino et al.*(2007)	*Pizones et al.*(2008b)	*Carrera et al.* (2005)

OFC: overall foam capacity, FC: foam capacity, CF: relative foam conductivity, MD: foam maximum density, $t_{1/2}$: foam half-life

Figure captions

Figure 1: Protein solubility and Z-potential values of silkworm protein concentrate (SPC) as a function of pH. Red horizontal line corresponds to Z-potential value equal to 0.

Figure 2: Sodium dodecyl sulphate polyacrylamide gel electrophoresis (SDS-PAGE) of silkworm protein concentrate (SPC) on the supernatant obtained at reconstitution pH and SPC supernatant following adjustment to pH 2.0 and 8.0.

Figure 3: Surface tension of silkworm pupae protein concentrate (SPC) as a function of protein concentration following completion of protein adsorption (24 h) at pH 2.0 and 8.0 (A), and the evolution of surface tension during protein adsorption until reaching a quasi-equilibrium value (B). Kinetic coefficients of protein adsorption are shown in (B) as inset. Different letters within a column indicate significant differences ($p < 0.05$).

Figure 4: Viscoelastic dilatational properties (E'_s and E''_s) of silkworm pupae protein concentrate (SPC) during protein adsorption at the A/W interface ($t < 180$ min) (A), and mechanical spectra obtained by means of frequency sweep tests (from 0.0075 to 0.1 Hz) for the SPC protein film formed at the A/W interface after reaching the pseudo-equilibrium state ($t > 180$ min) (B) at pH 2.0 and 8.0. Values represents the mean of three replicates. Standard deviation (SD) was plotted in some data points.

Figure 5: Viscoelastic properties (G'_s and G''_s) of silkworm pupae protein concentrate (SPC) obtained by interfacial small amplitude oscillatory shear (i-SAOS) measurements during protein adsorption at A/W interface ($t < 180$ s) (A), and mechanical spectra obtained by means of i-SAOS frequency sweep tests (from 0.0075 to 0.1 Hz) for the SPC protein film formed at the A/W interface after reaching the pseudo-equilibrium estate ($t > 180$ s) (B) at pH 2.0 and 8.0. Values represents the mean of three replicates. Standard deviation (SD) was plotted in some data points.

Figure 6: Foam volume decay curves of foams stabilized using silkworm protein concentrate (SPC) at pH 2.0 (A) and 8.0 (B). Values represents the mean of three replicates.

Figure 7: Macroscopic images and bubble size distribution of silkworm protein concentrate (SPC) foams at pH 2.0 showing the progress of the destabilization process over 800 s. Optical images were obtained with a CCD camera with a 2X objective coupled to FOAMSCAN device.

Supplementary Graph 1: Amplitude tests for dilatational experiments performed at 0.1 Hz after 90 min protein adsorption.

Supplementary Graph 2: Amplitude tests for interfacial shear experiments performed at 0.1 Hz after 90 min protein adsorption.

Table 1

Table 1: Proximate composition of the silkworm protein concentrate (SPC) before and after defatting.

	Before defatting	After defatting
Component	**% (w/w)**	**% (w/w)**
Protein	50.5 ± 1.0	71.0 ± 1.4
Lipid	28.9 ± 0.2	< 0.2
Carbohydrates*	5.1	7.2
Moisture	8.9 ± 0.1	12.5 ± 1.4
Ash	6.6 ± 0.8	9.3 ± 1.1

*Determined by difference

Table 2

Table 2: Ferric-reducing antioxidant power (FRAP) and oxygen radical absorbance capacity (ORAC) antioxidant activity of the protein concentrate obtained from the silkworm pupae (SPC) solubilized at pH 2.0 and 8.0. Values represent the mean of three independent replicates (n=3). Different letters within a column indicate significant differences ($p < 0.05$).

	Antioxidant activity (µmols Eq. Trolox·g^{-1} protein)	
pH value	**FRAP**	**ORAC**
pH 2.0	1659.2 ± 46.8^{a}	43.5 ± 8.1^{b}
pH 8.0	1826.0 ± 131.9^{a}	168.0 ± 3.0^{a}

Table 3

Table 3: Comparison of parameters obtained during foam formation and breakdown at pH 2.0 with other protein systems as previously reported in the literature using a FOAMSCAM device under the same operation conditions.

	Protein system			
Parameter	**Silkworm protein concentrate (SPC)**	**Sunflower**	**Sucrose/Soy Globulin**	**Sodium caseinate**
OFC (mL/s)	0.82 ± 0.03	0.8	0.8	1
FC	1.03 ± 0.02	1	0.8	0.8
CF (%)	28.2 ± 0.1	40	-	32
MD	0.10 ± 0.01	0.12	-	0.12
$t_{1/2}$ (s)	105 ± 3	400	250	-
Reference	*Present study*	*Patino et al.*(2007)	*Pizones et al.*(2008b)	*Carrera et al.* (2005)

OFC: overall foam capacity, FC: foam capacity, CF: relative foam conductivity, MD: foam maximum density, $t_{1/2}$: foam half-life

Figure captions

Figure 1: Protein solubility and Z-potential values of silkworm protein concentrate (SPC) as a function of pH. Red horizontal line corresponds to Z-potential value equal to 0.

Figure 2: Sodium dodecyl sulphate polyacrylamide gel electrophoresis (SDS-PAGE) of silkworm protein concentrate (SPC) on the supernatant obtained at reconstitution pH and SPC supernatant following adjustment to pH 2.0 and 8.0.

Figure 3: Surface tension of silkworm pupae protein concentrate (SPC) as a function of protein concentration following completion of protein adsorption (24 h) at pH 2.0 and 8.0 (A), and the evolution of surface tension during protein adsorption until reaching a quasi-equilibrium value (B). Kinetic coefficients of protein adsorption are shown in (B) as inset. Different letters within a column indicate significant differences ($p < 0.05$).

Figure 4: Viscoelastic dilatational properties (E'_s and E''_s) of silkworm pupae protein concentrate (SPC) during protein adsorption at the A/W interface ($t < 180$ min) (A), and mechanical spectra obtained by means of frequency sweep tests (from 0.0075 to 0.1 Hz) for the SPC protein film formed at the A/W interface after reaching the pseudo-equilibrium state ($t > 180$ min) (B) at pH 2.0 and 8.0. Values represents the mean of three replicates. Standard deviation (SD) was plotted in some data points.

Figure 5: Viscoelastic properties (G'_s and G''_s) of silkworm pupae protein concentrate (SPC) obtained by interfacial small amplitude oscillatory shear (i-SAOS) measurements during protein adsorption at A/W interface ($t < 180$ s) (A), and mechanical spectra obtained by means of i-SAOS frequency sweep tests (from 0.0075 to 0.1 Hz) for the SPC protein film formed at the A/W interface after reaching the pseudo-equilibrium estate ($t > 180$ s) (B) at pH 2.0 and 8.0. Values represents the mean of three replicates. Standard deviation (SD) was plotted in some data points.

Figure 6: Foam volume decay curves of foams stabilized using silkworm protein concentrate (SPC) at pH 2.0 (A) and 8.0 (B). Values represents the mean of three replicates.

Figure 7: Macroscopic images and bubble size distribution of silkworm protein concentrate (SPC) foams at pH 2.0 showing the progress of the destabilization process over 800 s. Optical images were obtained with a CCD camera with a 2X objective coupled to FOAMSCAN device.

Supplementary Graph 1: Amplitude tests for dilatational experiments performed at 0.1 Hz after 90 min protein adsorption.

Supplementary Graph 2: Amplitude tests for interfacial shear experiments performed at 0.1 Hz after 90 min protein adsorption.

Figure 1

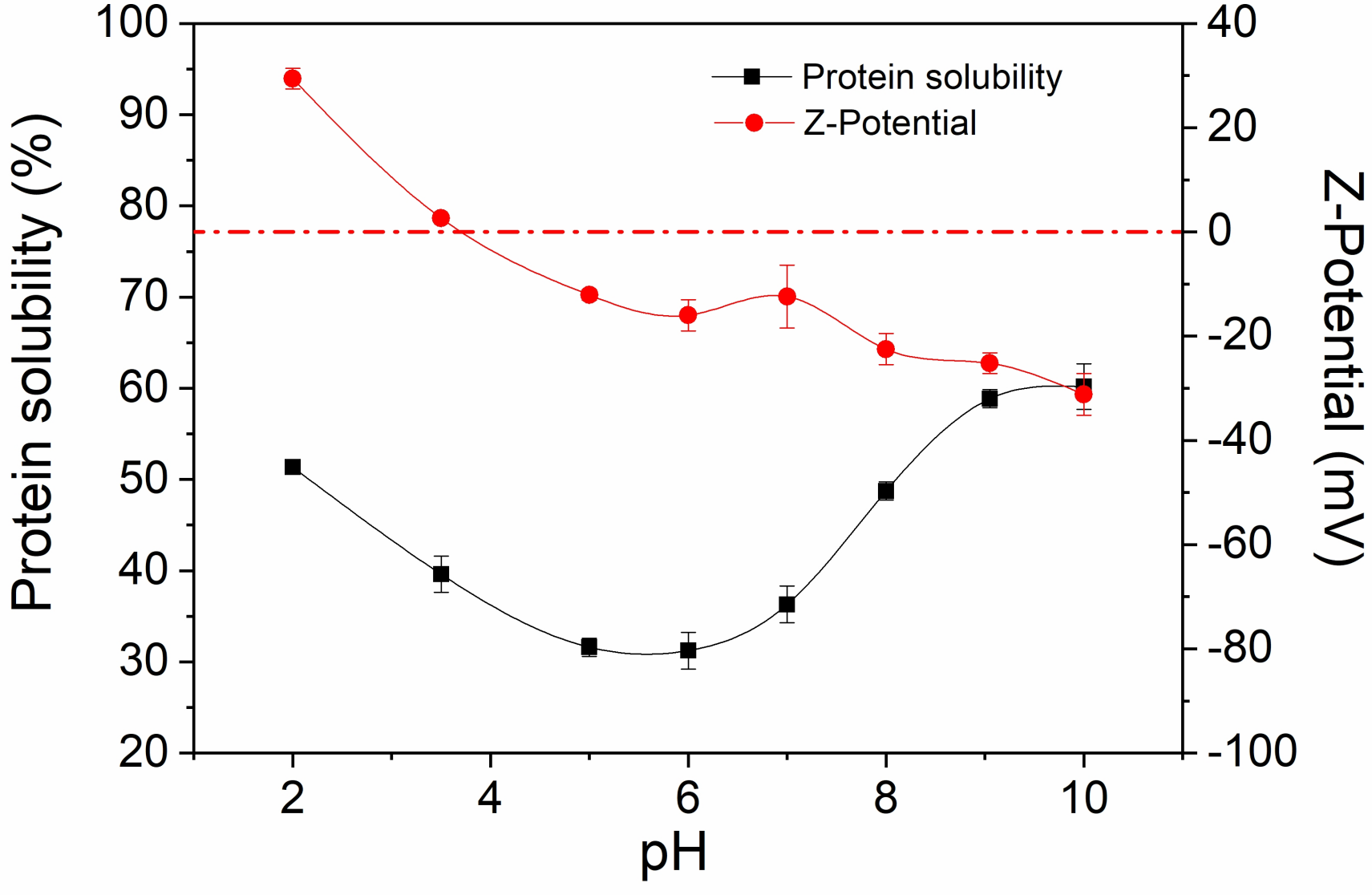
Protein solubility
Z-Potential
Protein solubility (%)
Z-Potential (mV)
pH
100
90
80
70
60
50
40
30
20
40
20
0
-20
-40
-60
-80
-100
2
4
6
8
10

Figure 2

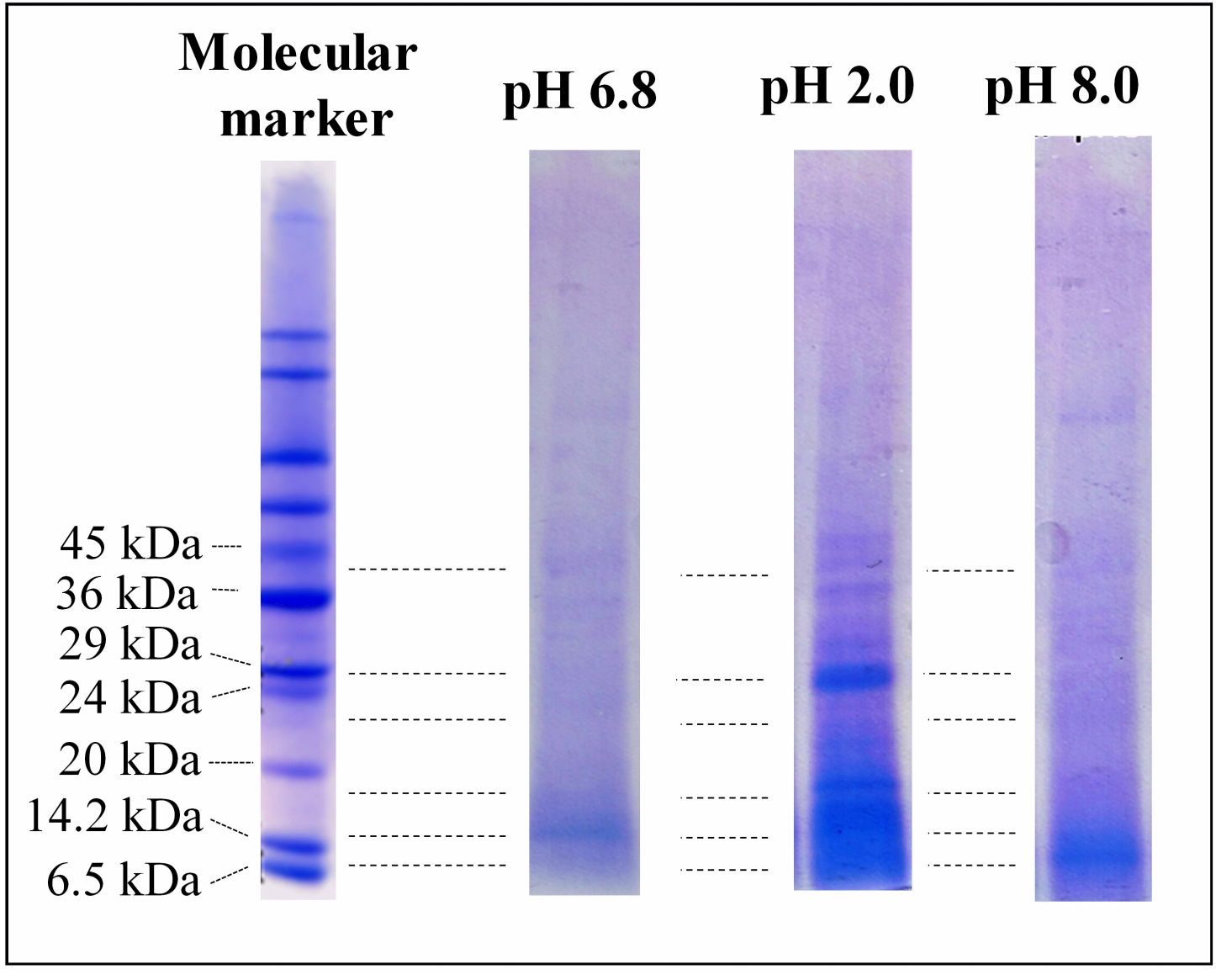
Molecular marker
pH 6.8
pH 2.0
pH 8.0
45 kDa
36 kDa
29 kDa
24 kDa
20 kDa
14.2 kDa
6.5 kDa

Figure 3

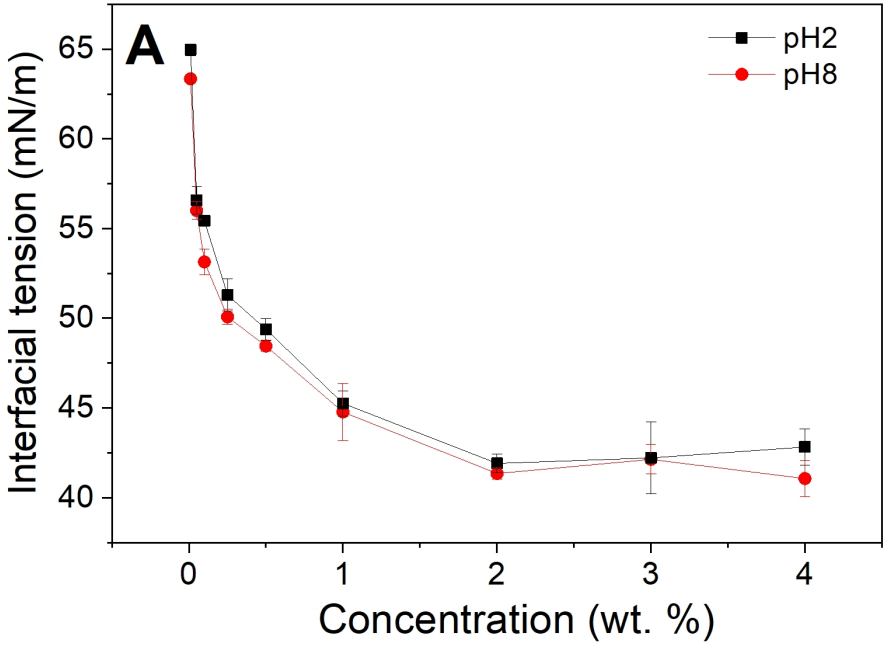
A
pH2
pH8
Interfacial tension (mN/m)
65
60
55
50
45
40
0
1
2
3
4
Concentration (wt. %)

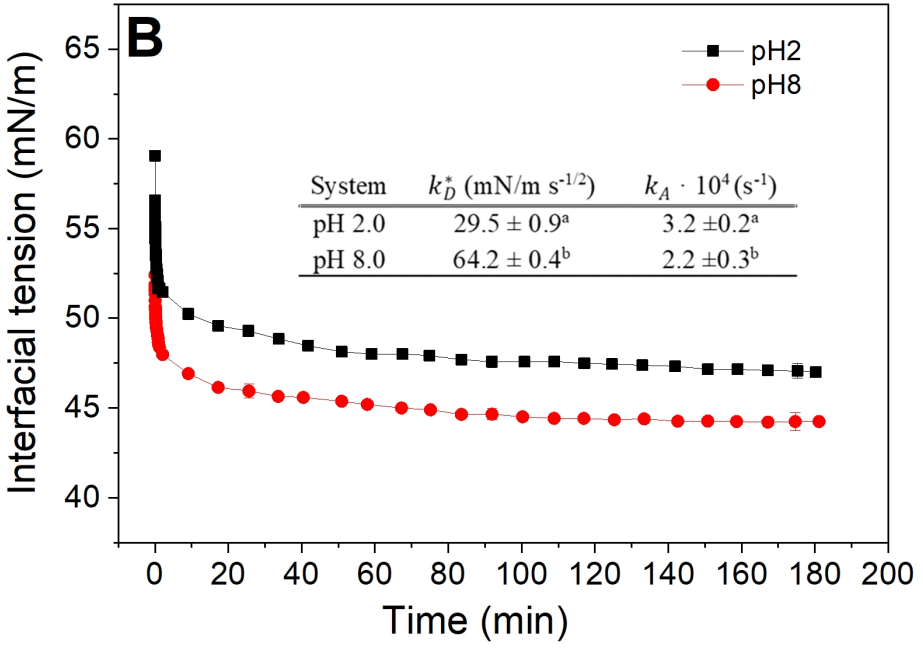
B
pH2
pH8
Interfacial tension (mN/m)
65
60
55
50
45
40
0
20
40
60
80
100
120
140
160
180
200
Time (min)
System
k_D^* (mN/m s$^{-1/2}$)
$k_A \cdot 10^4$ (s^{-1})
pH 2.0
29.5 ± 0.9^a
3.2 ±0.2^a
pH 8.0
64.2 ± 0.4^b
2.2 ±0.3^b

Figure 4

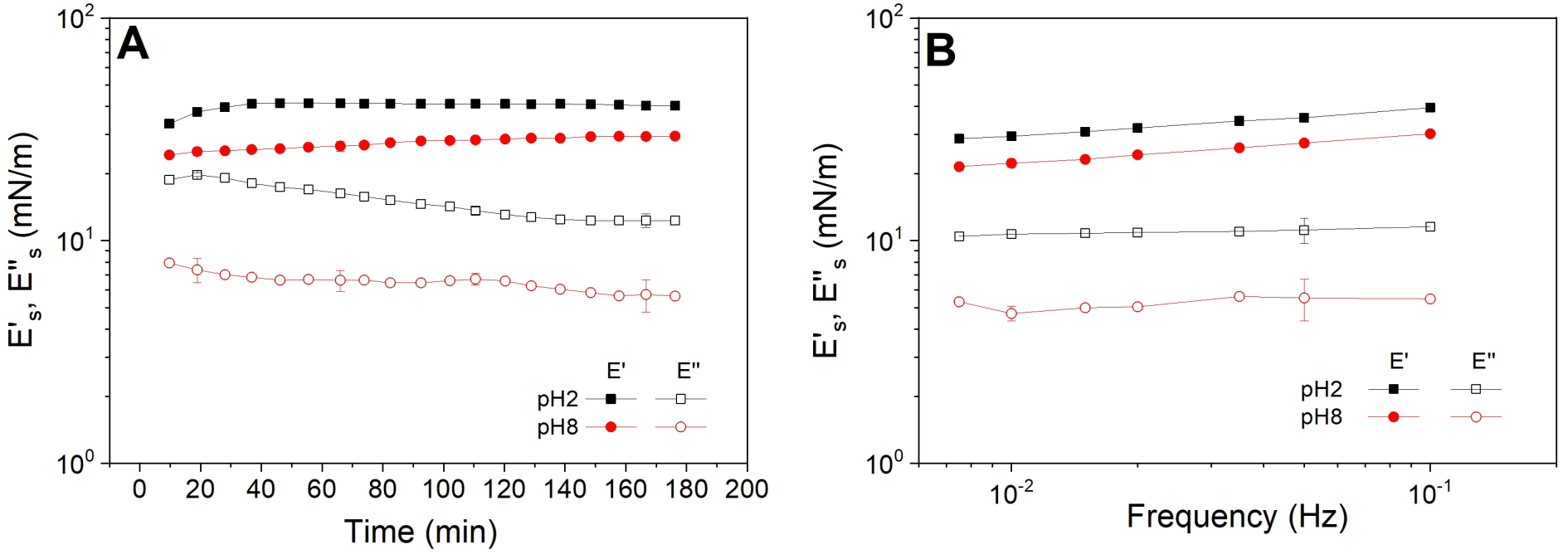
A
B
10^2
10^1
10^0
E'_s, E''_s (mN/m)
0 20 40 60 80 100 120 140 160 180 200
Time (min)
10^{-2}
10^{-1}
Frequency (Hz)
E'
E''
pH2
pH8

Figure 5

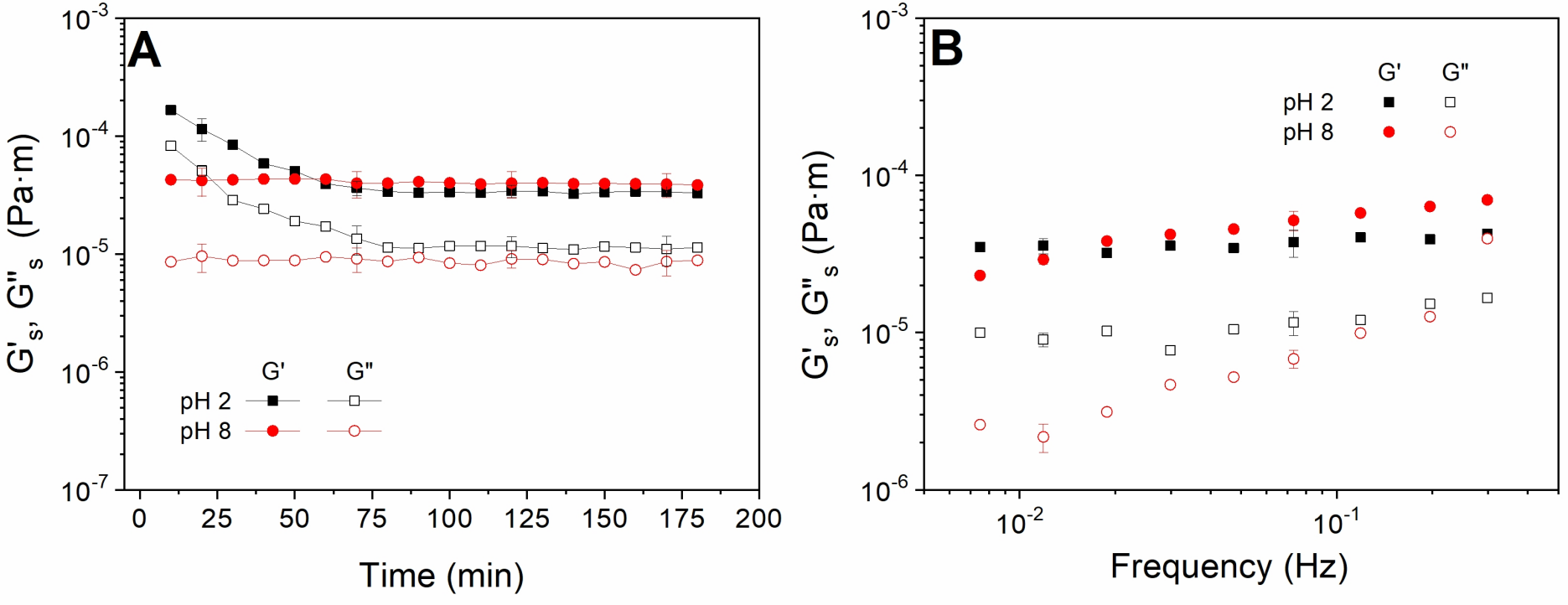

Figure 6

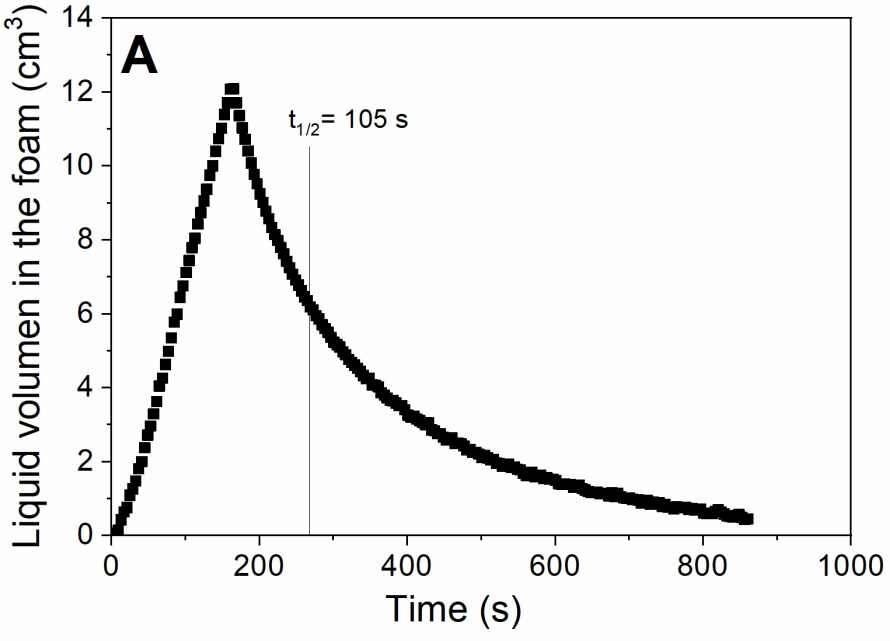
A
$t_{1/2}$= 105 s
Liquid volumen in the foam (cm^3)
Time (s)
0
2
4
6
8
10
12
14
0
200
400
600
800
1000

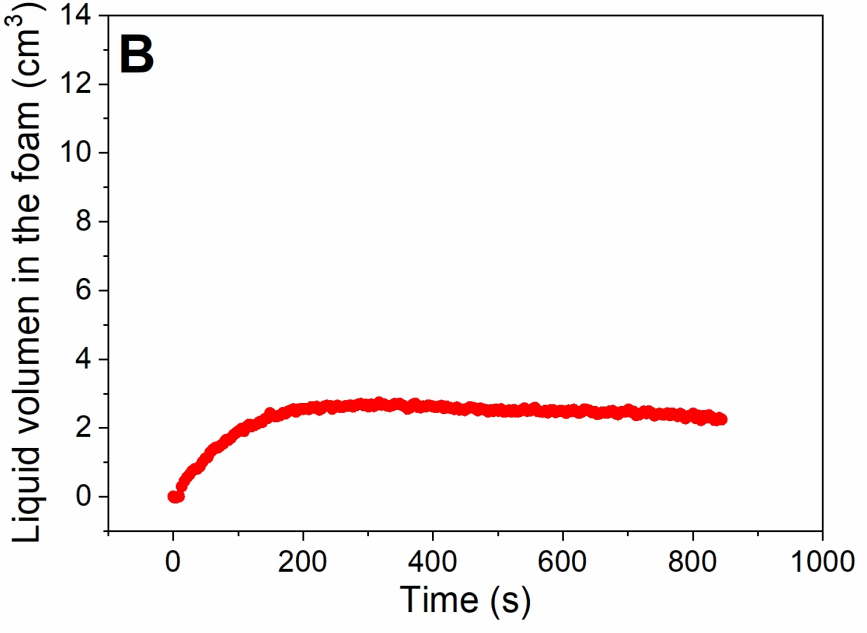
B
Liquid volumen in the foam (cm^3)
Time (s)
0
2
4
6
8
10
12
14
0
200
400
600
800
1000

Figure 7

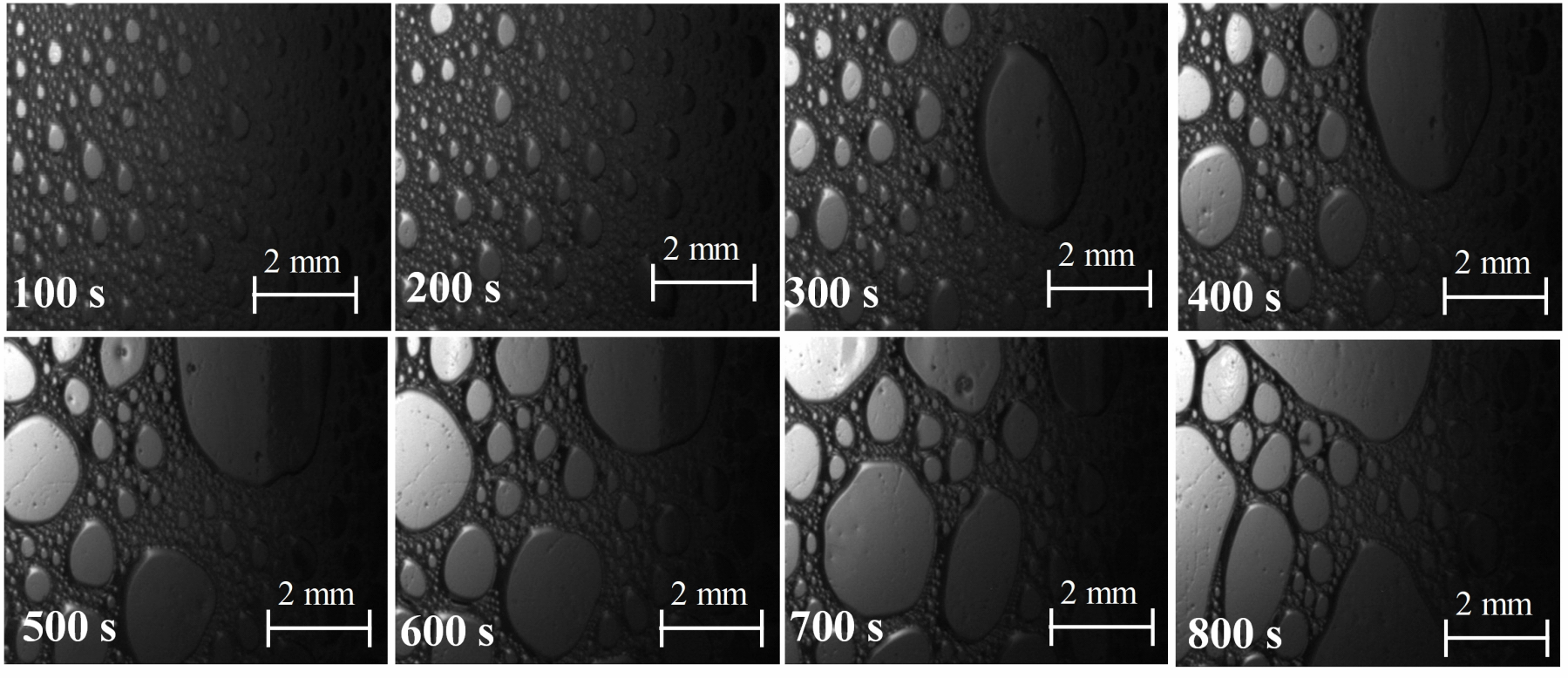
100 s
2 mm
200 s
2 mm
300 s
2 mm
400 s
2 mm
500 s
2 mm
600 s
2 mm
700 s
2 mm
800 s
2 mm

Suplementary Graph 1

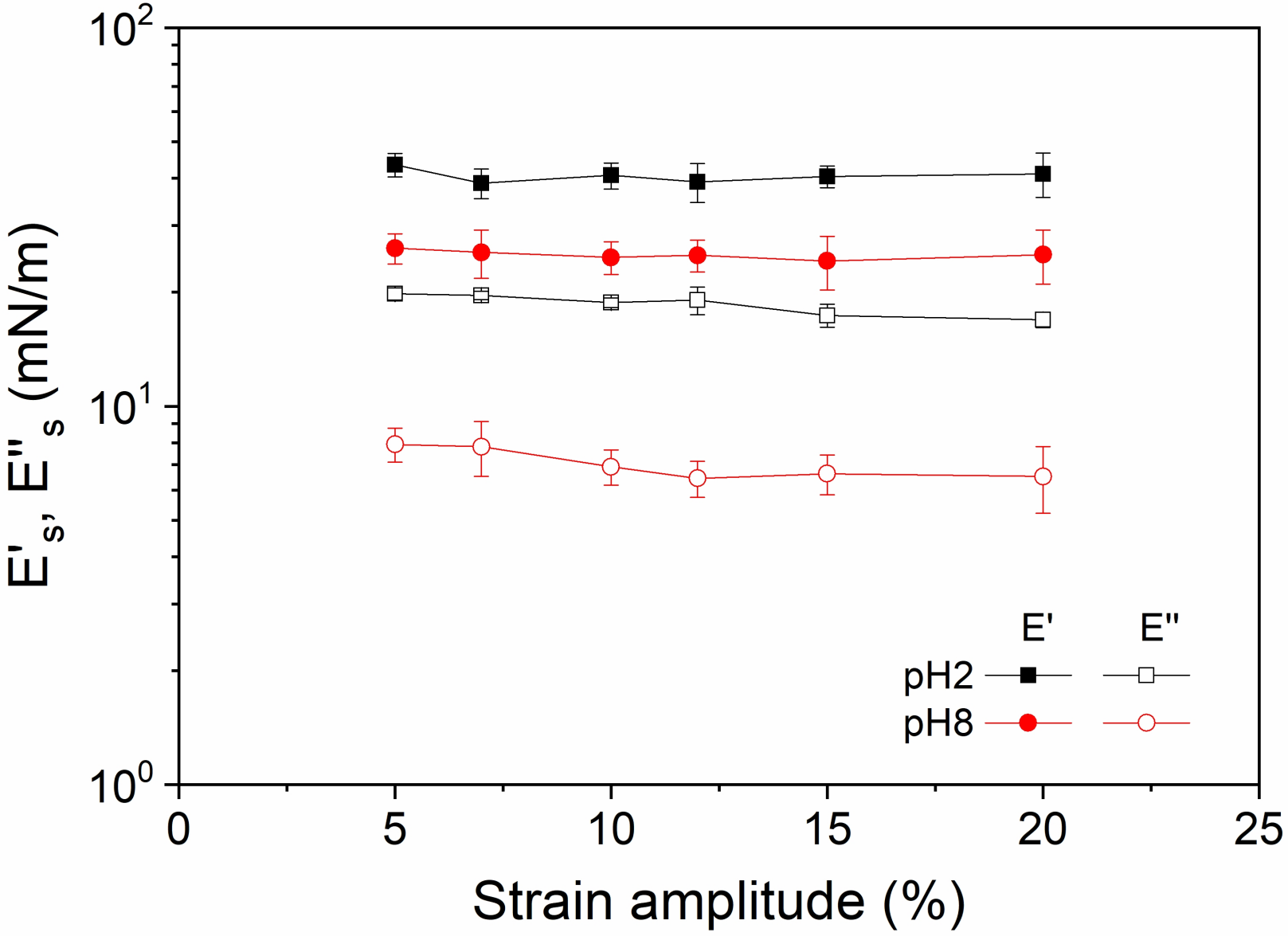

Suplementary Graph 2